Colloids and Surfaces B: Biointerfaces 104 (2013) 229–238

Colloids and Surfaces B: Biointerfaces

journal homepage: www.elsevier.com/locate/colsurfb

Biocompatibility of poly(lactic acid) with incorporated graphene-based materials

Artur M. Pinto[a,c], Susana Moreira[b], Inês C. Gonçalves[c,d], Francisco M. Gama[b], Adélio M. Mendes[a], Fernão D. Magalhães[a,*]

[a] LEPAE, Departamento de Engenharia Química, Faculdade de Engenharia, Universidade do Porto, Rua Roberto Frias, 4200-465 Porto, Portugal
[b] IBB – Institute for Biotechnology and Bioengineering, Centre of Biological Engineering, Universidade do Minho, Campus de Gualtar, 4710-057 Braga, Portugal
[c] INEB – Instituto de Engenharia Biomédica, Divisão de Biomateriais, Universidade do Porto, Rua do Campo Alegre, 823, 4150-180 Porto, Portugal
[d] Universidade do Porto, Faculdade de Engenharia, Departamento de Engenharia Metalúrgica e Materiais, Porto, Portugal

ARTICLE INFO

Article history:
Received 24 October 2012
Received in revised form
30 November 2012
Accepted 8 December 2012
Available online 21 December 2012

Keywords:
Topography
Wettability
Cytotoxicity
Platelets
Hemocompatibility

ABSTRACT

The incorporation of graphene-based materials has been shown to improve mechanical properties of poly(lactic acid) (PLA). In this work, PLA films and composite PLA films incorporating two graphene-based materials – graphene oxide (GO) and graphene nanoplatelets (GNP) – were prepared and characterized regarding not only biocompatibility, but also surface topography, chemistry and wettability. The presence of both fillers changed the films surface topography, increasing the roughness, and modified the wettability – the polar component of surface free energy increased 59% with GO and decreased 56% with GNP. Mouse embryo fibroblasts incubated with both fillers exceeded the IC_{50} in both cases with a concentration of 10 μg mL^{-1}. No variations in cell proliferation at the surface of the composite films were observed, except for those containing GO after 24 h incubation, which presented higher cell proliferation than pristine PLA films. Platelet adhesion to PLA and PLA/GNP films was lower in the presence of plasma proteins than when no proteins were present. Furthermore, incorporation of GNP into PLA reduced platelet activation in the presence of plasma proteins.

The results indicated that low concentrations of GO and GNP may be incorporated safely in PLA to improve aspects relevant for biomedical applications, such as mechanical properties.

1. Introduction

Aliphatic polyesters with reactive groups have attracted attention because of the demand of synthetic biopolymers with tuneable properties, including features such as hydrophilicity, biodegradation rates, bioadhesion, drug/targeting moiety attachment, etc. Poly(lactic acid) (PLA) has been widely investigated for biomedical applications because it is biodegradable, bioresorbable, and biocompatible [1,2]. This polymer has several applications in tissue and surgical implant engineering, like production of: bioresorbable artificial ligaments, hernia repair meshes, scaffolds, screws, surgical plates, and suture yarns [3,4]. PLA is also used in production of nano/microparticles for drug delivery, and in packaging of pharmaceutical products [5]. To make this material more attractive for some applications, as an effective alternative to petrochemical plastics, some properties should be improved, namely mechanical performance [6]. To attain these objectives different approaches have been tried according to the required applications. Some commonly used strategies are adjustment of crystallinity [7], incorporation of plasticizers [8], blends with other polymers [6] and addition of nanofillers. The latter is an interesting option, since with the addition of small weight percentages (wt.%) target properties can, in principle, be improved, while maintaining other key PLA properties intact. Good dispersion and interfacial interaction with the polymer matrix is paramount in order for these improvements to be significant. Most of the nanofillers reported are nanoclays [9], carbon nanotubes [10] and nanosilicas [11].

Graphene, the elementary structure of graphite, is an atomically thick sheet composed of sp^2 carbon atoms arranged in a flat honeycomb structure. It possesses remarkable mechanical strength and an extremely high surface area [12]. Since graphene is hydrophobic, stable dispersions in water can only be obtained with addition of proper surfactants [13]. Graphene oxide (GO) is similar to graphene, but presents oxygen-containing functional groups. The presence of these polar groups reduces the thermal stability of the nanomaterial, but may be important to promote interaction and compatibility with a particular polymer matrix [12,14].

GO and graphene have been reported as efficient drug carriers [15,16], as well as PLA [17]. Development of hybrid vehicles for drug targeting can take advantage of both materials properties and originate synergistic effects [18]. In addition, several graphene based biosensors are being developed [19]. Recent studies show

* Corresponding author. Tel.: +351 22 508 1601.
E-mail address: fdmagalh@fe.up.pt (F.D. Magalhães).

0927-7765/$ – see front matter © 2012 Elsevier B.V. All rights reserved.
http://dx.doi.org/10.1016/j.colsurfb.2012.12.006

that graphene substrates promote adherence of human mesenchymal stromal cells and osteoblasts [20], which can lead to better performance on tissues regeneration using scaffolds containing graphene and graphene oxide. Due to their great potential, several approaches are under study for future applications of these nanomaterials in biomedical engineering and biotechnology [21].

There are only a few studies regarding the biological effects of graphene and graphene derivatives [22–28]. Moreover, in some cases contradictory results are reported [22,28]. Some of the materials tested have identical designations, but in fact are obtained from different products and by different methods, leading to divergent conclusions. Most studies refer concentration dependent toxicity [23–26]. Effective mechanical reinforcement of polymeric materials using very small loadings of GO and graphene nanoplatelets (GNP) has been described by several authors [29–31]. Therefore, toxicological effects may not occur if the amount of nanofillers exposed or released from the polymer is sufficiently low to avoid attaining toxic concentrations.

The synthesis of GNP and GO does not require metal catalysis, contrarily to the production of carbon nanotubes, a chemically similar material that has attracted significant interest. Thus, cytotoxicity and inflammation caused by residual metals does not occur for GNP and GO [32].

An appropriate cellular response to implanted surfaces is essential for tissue regeneration and integration. It is well described that implanted materials are immediately coated with proteins from blood and interstitial fluids, and it is through this adsorbed layer that cells sense foreign surfaces. Although several studies have been made, it is not yet clear which material properties (e.g. topography, chemical composition, wettability, surface charge) favor in vitro protein adsorption and cell adhesion and proliferation [33]. Graphene and graphene oxide can affect protein adsorption and cell adhesion and proliferation, according to their intrinsic morphology and wettability. The adhesion and activation of platelets is also affected by the abovementioned factors. Presence of carbon nanotubes at the surface of PLA films was reported to decrease thrombogenicity [34]. In addition, the starting materials and methods used in the production of graphene-based materials, as well as the presence of toxic functional groups and contaminants, can affect biocompatibility.

In a previous study [35], we showed that incorporation of small amounts (0.4 wt.%) of GO and GNP in PLA significantly increases tensile strength and Young's modulus. Thus, this type of composites have a potential use in the production of surgical implants with improved mechanical performance. However, it is paramount to assure that these biomaterials do not present toxicity problems. In this work surface properties of PLA/GO and PLA/GNP thin films are characterized. Biocompatibility of the graphene-based fillers and composite films are evaluated through cytotoxicity and cell proliferation assays, respectively. Platelet adhesion and activation studies are used to assess hemocompatibility of the films.

2. Materials and methods

2.1. Materials and materials preparation

2.1.1. Materials

Poly(lactic acid) (PLA) 2002 D (4% D-lactide, 96% L-lactide content, molecular weight 121,400 g mol^{-1}), was obtained from Natureworks (Minnetonka, USA).

Graphene nanoplatelets (GNP) grade M5, were purchased from XG Sciences (Lansing, USA), with the following characteristics: average thickness of 6–8 nm, maximum length 5 μm, and surface area between 120 and 150 m^2 g^{-1}. GNP production is based on exfoliation of sulfuric acid-based intercalated graphite by rapid microwave heating, followed by ultrasonic treatment [36,37].

Carbon graphite micropowder, with purity above 99% and a diameter between 7 and 11 μm was purchased from American Elements, Los Angeles, USA.

2.1.2. Preparation of GO

Graphene oxide (GO) was prepared according to a modified Hummer's method. Briefly, 100 mL of H_2SO_4 were added to 3 g of graphite at room temperature and the solution was cooled using an ice bath, followed by gradual addition of 14 g of $KMnO_4$. Then 300 mL of distilled water were added, followed by addition of H_2O_2 (to reduce $KMnO_4$ excess) until oxygen release stopped. The solid was filtered and washed with water. After overnight resting, the resultant solution was decanted and the remaining product was centrifuged at 2000 rpm, during 5 min (this process was repeated four times). The solid was recovered and dried at 110 °C for 48 h [38].

2.1.3. Preparation of PLA/GO films

Nanocomposite thin films with GO and GNP were prepared by doctor blade casting of solvent dispersions, as described in a previous work [35]. GO was dispersed in acetone using an ultrasonic bath (Bandelin Sonorex RK 512 H) during 5 h and then added to a PLA/chloroform solution and again sonicated for 15 min. Concentration of GO relative to PLA was 0.4 wt.%, since in a previous work we have verified that this was the optimum loading for mechanical performance improvement in terms of tensile strength and Young's modulus [35]. Thin films (25–65 μm) were made by spreading the PLA/GO dispersion on a PTFE coated plate using a blade applicator. Solvent was completely removed by drying in a vacuum oven.

2.1.4. Preparation of PLA/GNP films

GNP were dispersed in chloroform using ultrasound sonication during 2 h and then dispersed in a PLA/chloroform solution. Concentration of GNP relative to PLA was 0.4 wt.%, for the abovementioned reason. Thin films (25–65 μm) were prepared and dried according to same procedures as the PLA/GO nanocomposites.

2.2. Films surface characterization

2.2.1. Contact angle and surface free energy measurements

A OCA 20 (Dataphysics) goniometer was used to measure the contact angles of ultrapure water, ethane-1,2-diol and hexadecane on pristine PLA, PLA/GO and PLA/GNP films, by sessile drop method. Data were collected with SCA 20 v2 software. Equilibrium contact angles (considered at 60 s) were measured for 5 μL droplet volumes. Determinations were made on 3 different locations for each condition.

The total surface free energy and the polar and dispersive components of the films were evaluated by the OWRK Method using SCA 20 software. Polar and dispersive components of the surface tension of the liquids that were used are 46.80 and 26.00 mN m^{-1} for water, 21.30 and 26.30 mN m^{-1} for ethane-1,2-diol and 0.00 and 27.47 mN m^{-1} for hexadecane, respectively.

2.2.2. Reflected light microscopy

Reflected light microscopy images of PLA, PLA/GO and PLA/GNP films were obtained with a Zeiss axiophot microscope, equipped with a Zeiss axiocam ICc 3. The specified spatial resolution is 370 nm.

2.2.3. X-ray photoelectron spectroscopy (XPS)

PLA, PLA/GO and PLA/GNP thin films and GNP, graphite and GO powders were analyzed with an Escalab 200 VG Scientific spectrometer working in ultra-high vacuum (1×10^{-6} Pa) and using

achromatic Al Kα radiation (1486.6 eV). The analyzer pass energy was 50 eV for survey spectra and 20 eV for high-resolution spectra. The spectrometer was calibrated using (Au $3d_{5/2}$ at 368.27 eV). The core levels for O 1s and C 1s were analyzed. The photoelectron take-off angle (the angle between the surface of the sample and the axis of the energy analyzer) was 90°. The electron gun used focused on the specimen in an area close to 100 mm^2. Analyzed samples were not conductive, for these reason spectra energy was displaced and a corrective shift based on the C 1s peak (285 eV) was performed. Curve fitting of the spectra was performed with the software XPS peak version 4.1.

2.2.4. Topography characterization

A stylus profilometer Hommel T8000, equipped with a pick-up-set taster TKL 300/17, was used to obtain a three-dimensional characterization of the topography of rectangular surface areas with 1.5 mm × 1.5 mm of PLA, PLA/GO and PLA/GNP films. Determinations were made on 3 different locations for each film. Roughness parameters determined were: S_a – arithmetic average height of the surface ($S_a = 1/A \int\int a \left|Z(x,y)\right| dxdy$, A – area) and S_p, S_v, and S_z which are parameters evaluated from the absolute highest and lowest points found on the surface, being: S_p – the maximum peak height, which is the height of the highest point; S_v – the maximum valley depth – which is the depth of the lowest point (expressed as a negative number); S_z – the maximum height of the surface. Thus, $S_z = S_p - S_v$ (ISO 25178-2) [39,40]. The specified space resolution is 100 nm in x, y and z.

2.3. In vitro biocompatibility assays

In vitro assays were performed using mouse embryo fibroblasts 3T3 (ATCC CCL-164), grown in Dulbecco's modified Eagle's media supplemented with 10% newborn calf serum (Invitrogen) and penicillin/streptomycin (1 mg mL^{-1}) (Sigma–Aldrich) [DMEM+], at 37.0 °C, in a fully humidified air containing 5% CO_2 (Infrared auto Flow). The cells were fed every 2–3 days. The cells were detached when 90% confluence was reached using a 0.25% (w/v) trypsin-EDTA solution (Sigma) and resuspended in culture medium at cellular density according to the assay. All assays were performed in triplicate and repeated at least 3 times. Results are presented as mean and standard deviation (SD).

2.3.1. Cell adhesion and proliferation on surface of PLA, PLA/GO and PLA/GNP films

Films (Ø 13 mm) constituted by PLA, PLA/GO and PLA/GNP were sterilized by immersion in ethanol (70%, v/v) and then washed with PBS (Phosphate Buffered Saline) before cells seeding at 5×10^4 cells/well and incubated. Polystyrene disc (PS) was used as positive control. Fibroblasts proliferation was evaluated using 1-(4,5-dimethylthiazol-2-yl)-3,5-diphenylformazan (MTT, Sigma), a colorimetric assay that gives a measure of the mitochondrial metabolic activity. Before the addition of MTT solution (0.5 mg mL^{-1} in PBS) films were changed to a new plate containing new medium. MTT assays were performed at 24, 48 and 72 h after cell seeded. The absorbance was measured at 570 nm and the cell proliferation inhibition index (CPII) was calculated using Eq. (1):

$$\text{CPII} = 100 - \frac{\text{DO}_{570\,\text{nm}} \text{ of test culture}}{\text{DO}_{570\,\text{nm}} \text{ of control culture (PS)}} \times 100 \quad (1)$$

2.3.2. Cytotoxicity evaluation of GO and GNP powders

Dry powders samples of GO and GNP were used to evaluate the graphene derivate cytotoxicity. Samples were sterilized by dissolution in ethanol (70%, v/v) and dried by solvent evaporation at room temperature under sterile conditions during 24 h, washed with PBS and then resuspended in DMEM at different concentrations. Cells were seeded onto 96-well plate at 5×10^3 cells/well. After 24 h of incubation the medium was removed and new medium containing the dispersed samples was added. Cell proliferation was evaluated trough MTT assay at 24, 48 and 72 h. Cells grown only in DMEM+ were used as control.

2.3.3. Direct contact assay

A fibroblast suspension containing 3×10^4 cells mL^{-1} was plated into each well of a six-well plate. After reaching a state of subconfluence (after 24 h), samples of PLA, PLA/GO and PLA/GNP films (Ø 13 mm) were placed on the wells, in direct contact with cells. After 48 h incubation, the cell morphology and viability was assessed, using the LIVE/DEAD® Viability/Cytotoxicity Kit for mammalian cells fluorescence (Invitrogen) labeling. Positive and negative controls (discs of latex and agar gel) were also used.

2.4. Platelet adhesion and activation

The adhesion of platelets to the surface of Ø 14 mm disks of PLA, PLA/GO and PLA/GNP films were evaluated by counting and observation of morphological features using scanning electron microscopy (SEM). Wells of 24-well plates were blocked by adding BSA (bovine serum albumin) 1% (w/v) in each well followed by 1 h incubation at 37 °C, and then rinsing with PBS (0.01 M, pH 7.4). Films were sterilized in ethanol 70% (v/v) for 20 min, and then rinsed with PBS. To evaluate the effect of serum proteins in platelet adhesion and activation, the samples, PS [poly(styrene)] – control, PLA, PLA/GO and PLA/GNP were first incubated with two different pre-immersion solutions: PBS or human plasma 1% (provided by the Portuguese Blood Institute) in a 24-well plate for 30 min at 37 °C, and afterwards rinsed with PBS. The human platelets concentrate (PC) (obtained from the Immunohemotherapy service – Hospital S. João, Porto, Portugal) was diluted in PBS to a concentration of 3×10^8 platelets mL^{-1}. Samples were incubated with the freshly prepared PC in the previously blocked 24-well plates for 30 min at 37 °C under 90 rpm. Finally, the samples were rinsed with PBS. Adherent platelets were fixed with freshly prepared solution of 1.5% glutaraldehyde (Merk) in 0.14 M sodium cacodylate buffer (Merk) for 30 min at room temperature and then rinsed with PBS. Afterwards, the samples were dehydrated with a growing ethanol/water gradient, for 10 min each: 50, 60, 70, 80, 90 and 99% (v/v). Next, 100 μL of hexamethyldisilazane (Sigma–Aldrich) were added to each well and the samples were left to dry in the hoot overnight. Finally, the samples were sputtered with a conductive gold/palladium layer and observed by SEM (FEI Quanta 400FEG) at CEMUP – Centro de Materiais da Universidade do Porto. The degree of activation was evaluated by qualitative observation of the platelets morphology. Two degrees were considered: (a) non-activated and (b) activated (see Fig. 1). Platelets were considered activated if they had more than one pseudopod or were fully spread (Fig. 1C and D).

Samples were pre-immersed in PBS or plasma. At least 10 samples were used to calculate mean and standard deviation for each material in each pre-immersion condition.

2.5. Statistical analysis

Statistical analysis was made by analysis of variance (ANOVA). Multiple means comparison was performed between samples to identify significant differences, which were considered for $p < 0.05$. In suitable cases independent two samples Student's t-test was used. Significant differences were also considered for $p < 0.05$.

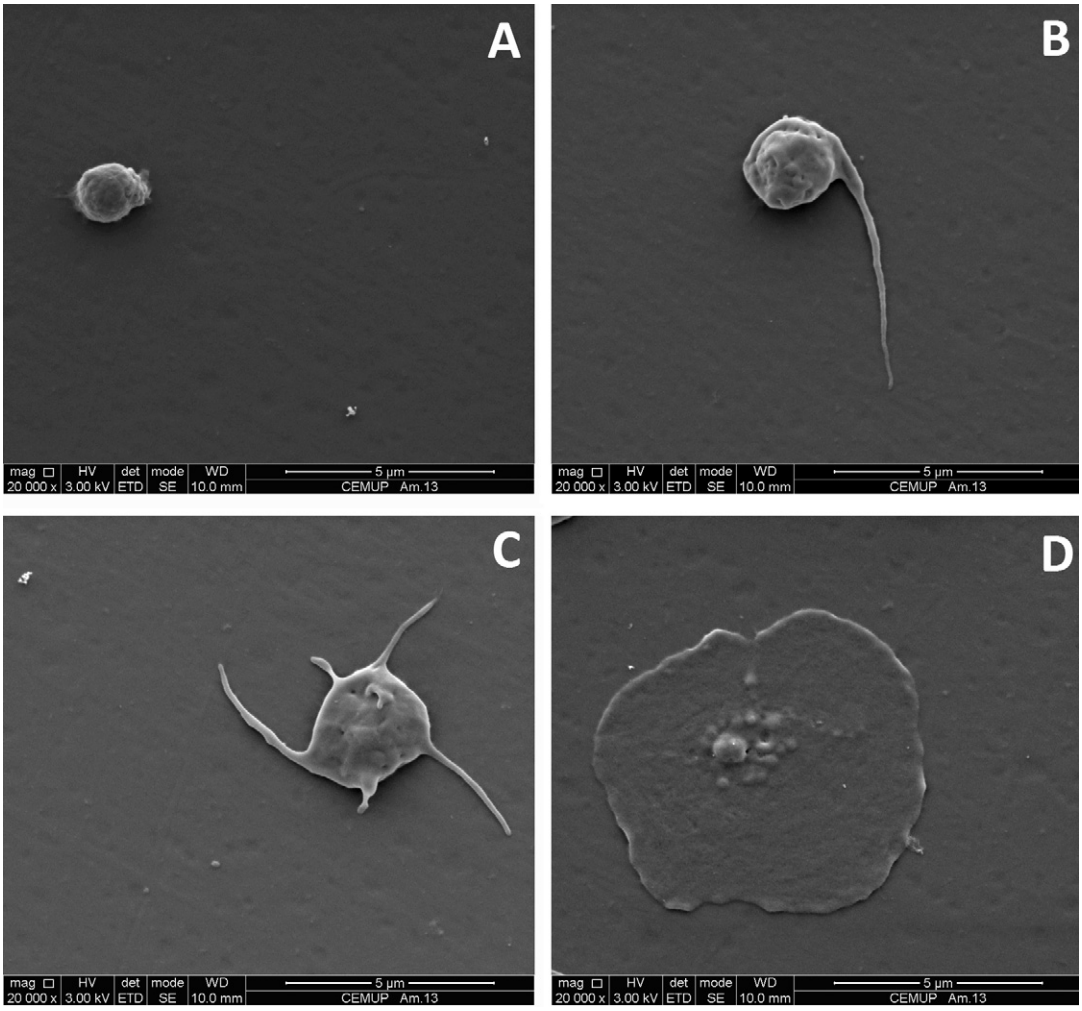

Fig. 1. Activation degree of platelets at the surface of the films. Representative images of non-activated (A and B) and activated (C and D) platelets, at 20,000× magnification.

3. Results and discussion

3.1. Topographical characterization

The 3D topography images shown in Fig. 2 compare the surfaces of pristine PLA films with PLA/GO and PLA/GNP composite films surfaces. The peaks seen in Fig. 2B correspond to agglomerates (1–2 μm), since individual GO sheets are too small to be detected by this technique (sizes in the order of tenths of micron) [35]. On the other hand, GNP particles have nominal lengths close to 5 μm, allowing for the observation of both individual and agglomerated particles (Fig. 2C). The peaks are distributed throughout the entire surface. A grooved pattern was observed on the surfaces of all samples. Reflected light microscopy was used to identify the cause of this pattern (discussed next).

Table 1 shows that films with GO and GNP incorporation present higher positive values of S_p and S_t than pristine PLA films, due to presence of fillers at the surface. PLA/GNP films presented negative values of S_v higher than PLA/GO films. This may be an indication of GNP having less compatibility with the polymer matrix than GO, thus being less embedded in it, existing more pronounced depressions surrounding GNP than GO particles. GO has more functional groups with oxygen than GNP (shown in Section 3.2), which form hydrogen bonds with similar groups in PLA. Differences in S_a between samples are not considerable because only a very small weight percentage of nanofillers are dispersed in the films.

Reflected light microscopy images (Fig. 3) show that the surface of the films presents grooves with pitches between 0.5 and 2 μm for all conditions. These grooves are in the same direction as the spreading of the films. This might occur due to imprinting of a micropattern present in the doctor blade during spreading. Rapid solvent evaporation in these thin films hinders surface leveling and originates this morphology. GO and GNP are visible in Fig. 3B and C as dark and bright spots, respectively.

3.2. Chemical characterization

Chemical properties of nanofillers used in a composite are relevant in two important contexts: (i) compatibility with the polymer matrix, and (ii) biological effects when exposed at the film surface

Table 1
Roughness parameters for PLA, PLA/GO and PLA/GNP films. S_a – arithmetic average height of the surface, S_p – maximum peak height, S_v – maximum valley depth, S_z – maximum height of the surface. Results are presented as mean and standard deviation (in parenthesis) for $n = 3$.

Samples	Roughness parameters			
	S_a (nm)	S_p (nm)	S_v (nm)	S_z (nm)
PLA	43 (11)	730 (124)	−711 (427)	1441 (346)
PLA/GO	43 (6)	1623 (370)	−816 (203)	2439 (565)
PLA/GNP	37 (6)	1211 (476)	−1797 (963)	3008 (1424)

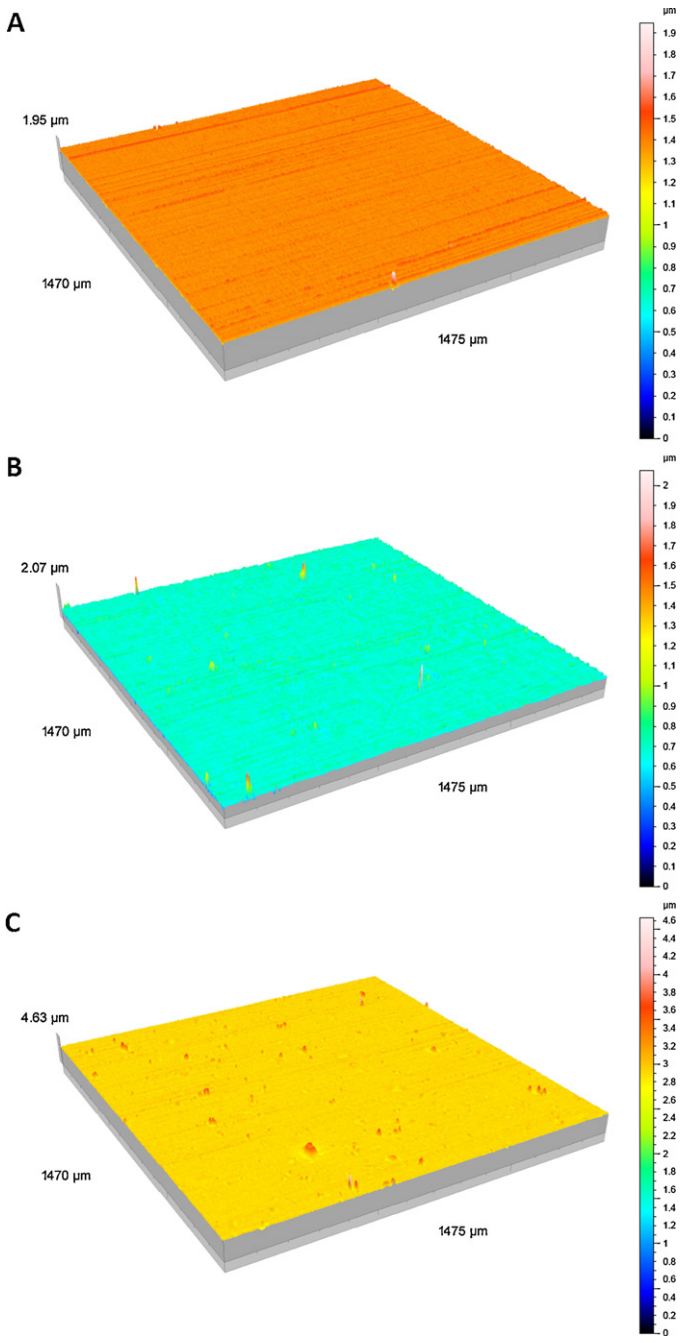

Fig. 2. Representative 3D images of the topography of the surface of pristine PLA (A), PLA/GO (B) and PLA/GNP (C) films.

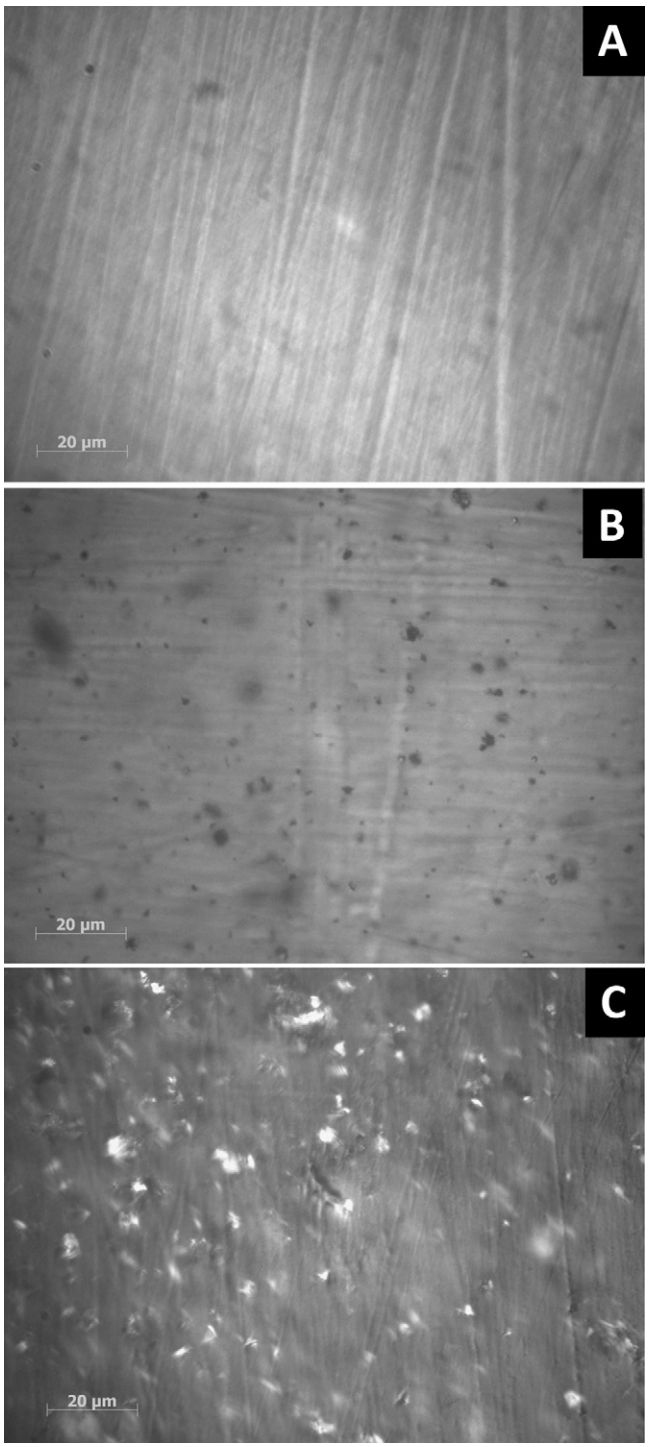

Fig. 3. Reflected light microscopy of the surface of PLA (A), PLA/GO (B) and PLA/GNP (C) films.

or released due to matrix biodegradation. XPS results (Fig. 4 and Table 2) show that, both graphite and GNP present a low degree of oxidation (atomic percentage of oxygen – O 1s (at.%) < 9%). This was expected since graphite is mainly constituted by carbon atoms and GNP is obtained from graphite by microwave and ultrasonic treatment (see Section 2.1.1). XPS data also reveal that oxidation of graphite by modified Hummer's method, to produce graphene oxide, increases the O 1s (at.%) in the final product (GO) by about 15%. The most ubiquitous oxygen functional groups identified in GO are ethers.

Table 2
Atomic composition of graphite, GNP and GO, determined by XPS. Results are presented as mean and standard deviation (in parenthesis).

Sample	C 1s (at.%)	O 1s (at.%)
GNP	92.4	7.6
Graphite	91.7	8.3
GO	78.3	21.7

Concerning the composite films, the C and O 1s (at.%) at the surface of PLA, PLA/GO and PLA/GNP films are similar for every condition (Table 3). Major oxygen containing functional groups identified for the three cases were ethers and carbonyls. Again there were no considerable differences between the films. This might

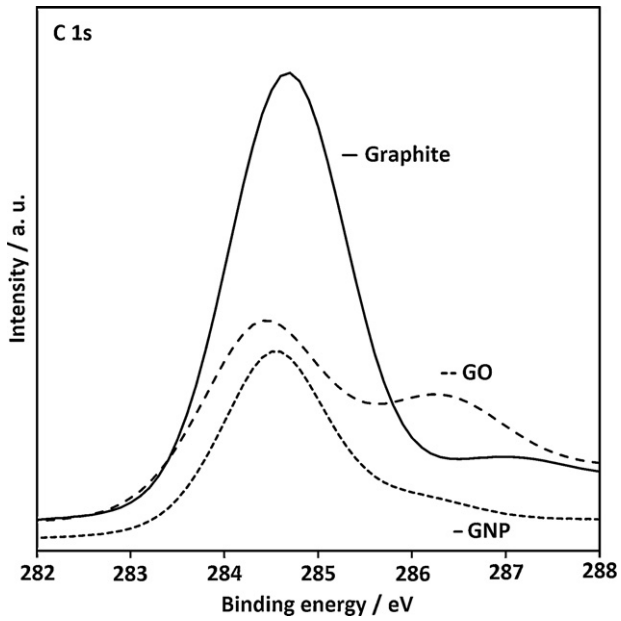

Fig. 4. XPS spectra for the core level C 1s (after fitting) of graphite, GO and GNP powders.

happen because the contribution of the filler (at a loading of only 0.4 wt.%) to the final C and O 1s (at.%) cannot be detected by XPS.

3.3. Wettability of films surface

Contact angle measurements (Table 4) show that the water contact angle of PLA/GO films decreased about 9° comparing with pristine PLA films. This shows that the presence of GO at the film surface increases its hydrophilicity. Hydrogen bond interactions between oxygen-containing groups in GO and water can explain this behavior. Hexadecane completely wetted the surface of PLA/GO films (Fig. 5E), while at the surface of pristine PLA films it presented a contact angle close to 27°. Hydrophobic interactions with hexadecane might be established with the honeycomb sp^2 carbon atoms. This suggests that the presence of GO particles induces an amphiphilic behavior of the surface.

Table 3
Atomic composition analysis by XPS of the surface of PLA, PLA/GO and PLA/GNP films. Results are presented as mean and standard deviation (in parenthesis) for $n = 3$.

Sample	C 1s (at.%)	O 1s (at.%)
PLA	62.1 (2.36)	37.9 (2.36)
PLA/GNP	63.7 (2.73)	37.8 (2.63)
PLA/GO	61.7 (0.74)	38.3 (0.74)

Table 4
Contact angles at 60 s of H_2O, ethane-1,2-diol and hexadecane on PLA, PLA/GO and PLA/GNP films. Results are presented as mean and standard deviation (in parenthesis) for $n = 3$.

Samples	Contact angles (°)		
	H_2O	Ethane-1,2-diol	Hexadecane
PLA	87.2 (0.36)	56.9 (2.14)	26.7 (3.37)
PLA/GO	78.1 (2.06)	55.2 (3.38)	0 (0.00)
PLA/GNP	89.6 (0.97)	65.3 (0.94)	0 (0.00)

The water contact angle of PLA/GNP film increased 2.3°, comparing to pristine PLA films, showing a small hydrophobic effect. As occurred for PLA/GO films, hexadecane completely wetted the surface of PLA/GNP films (Fig. 5D). However, the contact angle for ethane-1,2-diol increased, probably due to the presence of much less oxygen functional groups in GNP particles than in GO sheets at the film surface.

All the above mentioned findings suggest that the presence of the fillers at the film surface, despite not changing the surface composition significantly (shown in Section 3.2), affect its wettability. This might occur because of direct interaction of the liquids with partially exposed fillers at the PLA surface. Wang and co-workers measured water contact angles on poly(vinyl alcohol)/graphene

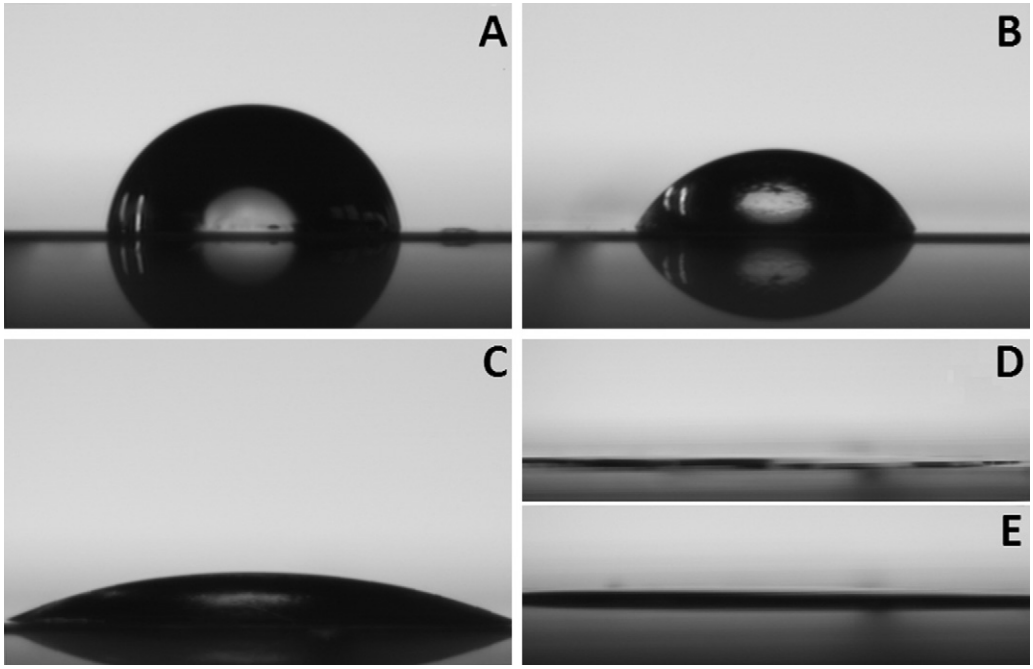

Fig. 5. Contact angle images for: A – water on PLA, B – ethane-1,2-diol on PLA, C – hexadecane on PLA, D – hexadecane on PLA/GO and E – hexadecane on PLA/GNP film surface.

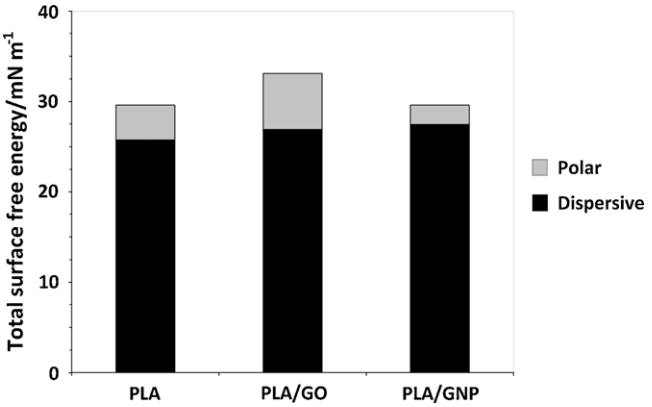

Fig. 6. Dispersive and polar components of the total surface free energy of PLA, PLA/GO and PLA/GNP films.

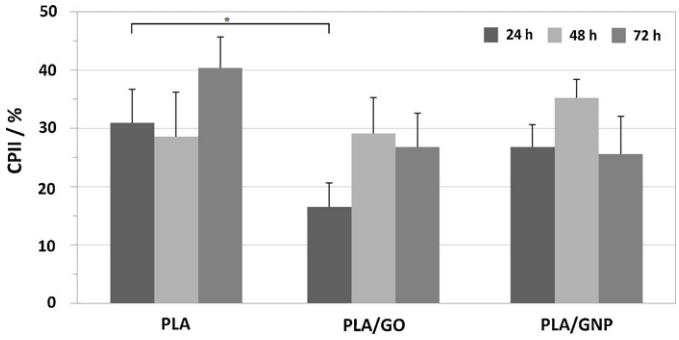

Fig. 7. Cell proliferation inhibition index for mouse embryo fibroblasts, cultured on PLA, PLA/GO and PLA/GNP films. Results are presented as mean and error bars represent SD. *Significantly different ($p < 0.05$).

dry films and observed that 0.5 wt.% graphene loading increased the contact angle from 36° to 93° [41].

Fig. 6 shows surface free energy values computed from the contact angle measurements. The total surface free energy of PLA increases about 12% with the incorporation of 0.4 wt.% GO. However, for the same incorporated amount of GNP, no changes are observed. Additionally, as expected, the polar component of PLA films increases about 59% with addition of GO and decreases 56%

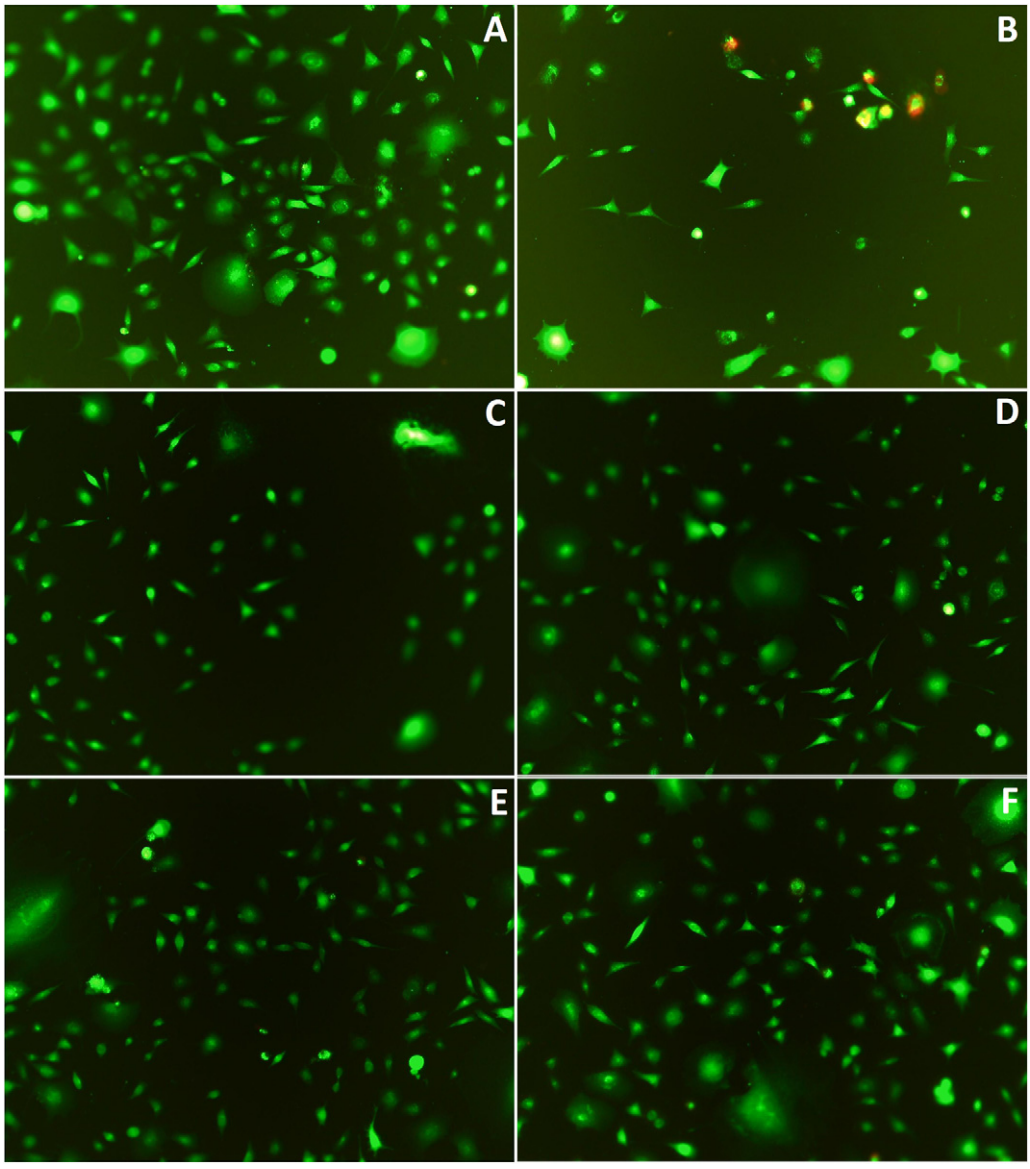

Fig. 8. Fluorescence microscopy of mouse embryo fibroblasts after 48 h incubation in the direct contact assay: A – Agar (negative control); B – positive control (latex rubber); C and D – PLA; E – PLA/GO and F – PLA/GNP. (For interpretation of the references to color in the text, the reader is referred to the web version of the article.)

with incorporation of GNP. These results are in accordance with the discussion presented above for the contact angles.

3.4. In vitro biocompatibility assessment

In order to evaluate the cytotoxicity of the films, we have studied the effects of these materials in a mouse embryo fibroblast culture, namely in terms of cell adhesion and proliferation on the films, morphological features and cell death.

After 24 h of culture, fibroblasts adhesion and proliferation on the PLA/GO films (CPII ca. 17%) was significantly higher than for pristine PLA (CPII ca. 31%) ones ($p < 0.05$) (Fig. 7). This can be due to the presence of GO at the surface increasing its hydrophilicity or creating a more suitable surface morphology for protein adsorption and cell adhesion. Higher surface hydrophilicity favors vitronectin adhesion and allows the maintenance of fibronectin functionality. Furthermore, cell proliferation requires the reorganization of surface-adsorbed fibronectin, which occurs in hydrophilic surfaces and is often impaired in more hydrophobic surfaces. Increase in surface roughness may lead to higher fibronectin adsorption due to the increase of surface area [33]. Interestingly, Ruiz et al. [28] observed that mammalian colorectal adenocarcinoma HT-29 cells attached and proliferated more efficiently in GO coated glass slides, than in control (glass slides). After 48 and 72 h, the proliferation rate at the surface of PLA/GO films seems to decrease and no significant differences are observed comparing to PLA films ($p > 0.05$). Also, no significant differences ($p > 0.05$) are observed in CPII between PLA and PLA/GO comparing to PLA/GNP films, until 72 h. Thus, the presence of GNP at films surface does not seem to affect cell adhesion and proliferation.

Yoon et al. reported that the proliferation and viability of neuronal cells (PC 12) on poly(D,L-lactic-co-glycolic acid) [PLGA]/GO (2 wt.%) nanocomposite scaffolds increased by 8% in comparison to pristine PLGA scaffolds [42]. However, Lahiri et al., showed that the viability of osteoblasts (ATCC, Manassas, VA, USA) grown at the surface of ultra-high molecular weight poly (ethylene)–GNP nanocomposite films (0.1 wt.%) decreased about 6, 14 and 17% comparing to pristine polymer after, respectively, 1, 3 and 5 days of incubation [25].

The cytotoxicity of the films was also assessed using a direct contact method. For that purpose the films were used together with a positive and negative control (latex rubber and agar, respectively). Each sample was placed on top of a sub-confluent cellular layer on a six-well plate, as described in the material and methods section.

Fig. 8 shows the results obtained with the fluorescence labeling of the cell layers. As expected, the latex rubber is cytotoxic. Thus, the majority of cells were floating in the medium and some of those that remained attached were also dead (red labeled – Fig. 8B). No differences in morphology were found for the cells on the films surface and on the negative control (agar – Fig. 8A). Moreover, all of the cells remained alive, as shown by the green fluorescence (Fig. 8A and C–F). These results suggest that films can be considered non-toxic.

In a previous work we observed that PLA/poly(caprolactone) composite loses 10% of its mass after 16 weeks of hydrolytic degradation [43]. Although the degradation rate is quite slow, we accessed the cytotoxicity of the nanofillers alone, in order to evaluate potential leaching-related effects. Mouse embryo fibroblasts were incubated with different GO and GNP concentrations, and cell proliferation evaluated.

Fig. 9, shows that CPII increased with the increase of GO/GNP concentrations tested (1–10 $\mu g\,mL^{-1}$). It has been reported that nanofillers such as GO might induce the formation of reactive oxygen species [23], which could explain this decrease on cell proliferation. Nevertheless, there are no significant differences between GO and GNP for every concentration and incubation time

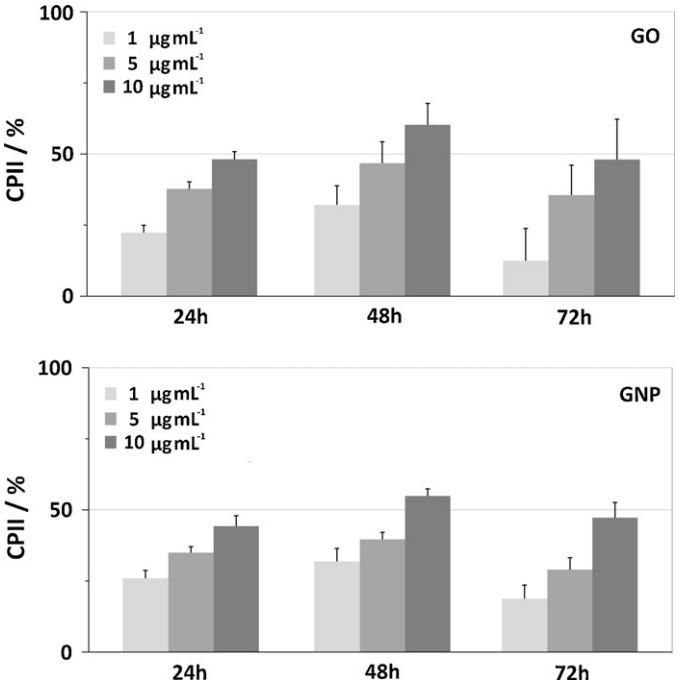

Fig. 9. CPII of mouse embryo fibroblasts after incubation with GO and GNP powders in concentrations from 1 to 10 $\mu g\,mL^{-1}$ along time. Results are presented as mean and error bars represent standard deviation.

tested ($p > 0.05$). For both materials, IC_{50} is exceeded with concentrations of 10 $\mu g\,mL^{-1}$.

Wojtoniszak et al. showed that the viability of L929 cells decreased to 36.3% when exposed to GO functionalized with poly (ethylene glycol) [PEG] at 100 $\mu g\,mL^{-1}$. Also, cells exposed to the suspension of RGO/PEG at concentrations between 3 and 25 $\mu g\,mL^{-1}$ showed relatively high viability. However, when the concentration exceeded 25 $\mu g\,mL^{-1}$, viability diminished abruptly [26]. Results from Chang et al. suggest that GO do not enter A549 cells, and no obvious cytotoxicity was observed even for the higher concentration tested (200 $\mu g\,mL^{-1}$). But GO can cause a dose-dependent oxidative stress in cell and induce a slight loss of cell viability at high concentration (200 $\mu g\,mL^{-1}$) [23].

Considering that the concentration of interest of nanofillers in PLA/GO and PLA/GNP films is very low and that the polymer degradation rate is slow, the concentrations of these graphene derived materials at the nanocomposites/cells interface or in the physiological medium as the material degrades are not expected to reach values that significantly inhibit cell proliferation (Figs. 7 and 8).

3.5. Platelet adhesion and activation

Since PLA is a biomaterial commonly used in surgery (e.g. orthopedy, dental medicine, hernia repair meshes), it should present low thrombogenicity in order to prevent the formation of post-operative blood cloths [5]. Adhesion and activation of platelets at the surface of PLA, PLA/GO and PLA/GNP films were evaluated by counting and qualitative observation of morphological features using SEM (see Section 2.4). To evaluate the effect of serum proteins on platelet adhesion and activation the samples were pre-immersed either in PBS or human plasma 1%. Fig. 10 shows that significantly less ($p < 0.05$) platelets adhered to PLA and PLA/GNP when samples were previously treated with human plasma comparing to those pre-immersed in PBS. This may occur due to adsorption of non-thrombogenic proteins, such as albumin, at the surface of the films preventing platelet adhesion. Moreover, when in presence of plasma proteins, the number of activated

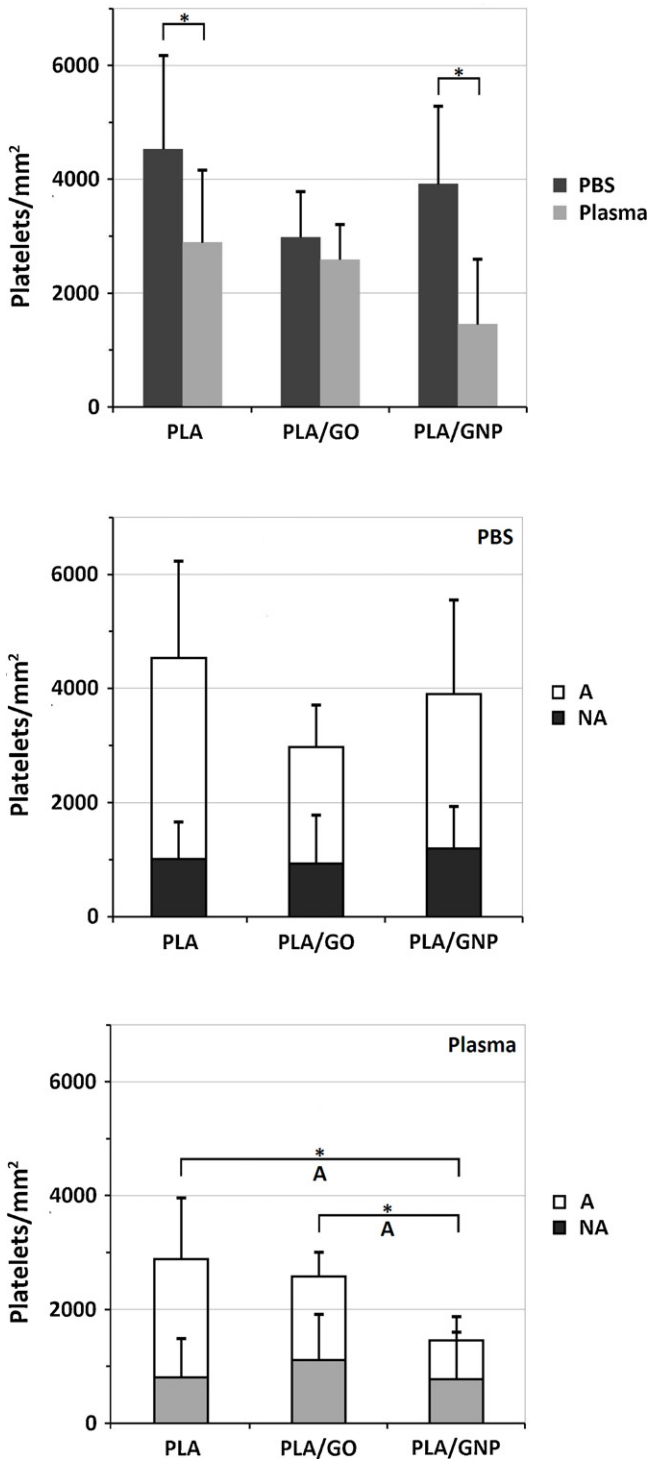

Fig. 10. Platelet adhesion on PLA, PLA/GO and PLA/GNP films surface, pre-immersed in PBS or plasma. Degree of activation of the platelets adhered to the surface of the films pre-immersed in PBS or in plasma. A – activated, NA – non activated. Results are presented as mean and error bars represent standard deviation. *Significantly different ($p < 0.05$).

platelets in PLA/GNP films is significantly lower ($p < 0.05$) than that in PLA and PLA/GO films (Figs. 10 and 11). This can be explained by the presence of hydrophobic GNP (see Section 3.3) at the surface of the films, favoring protein adsorption at the material surface. This blocks platelet activation in case of these proteins being albumin, which is generally the first to adhere because of its abundance in plasma and its small size [44].

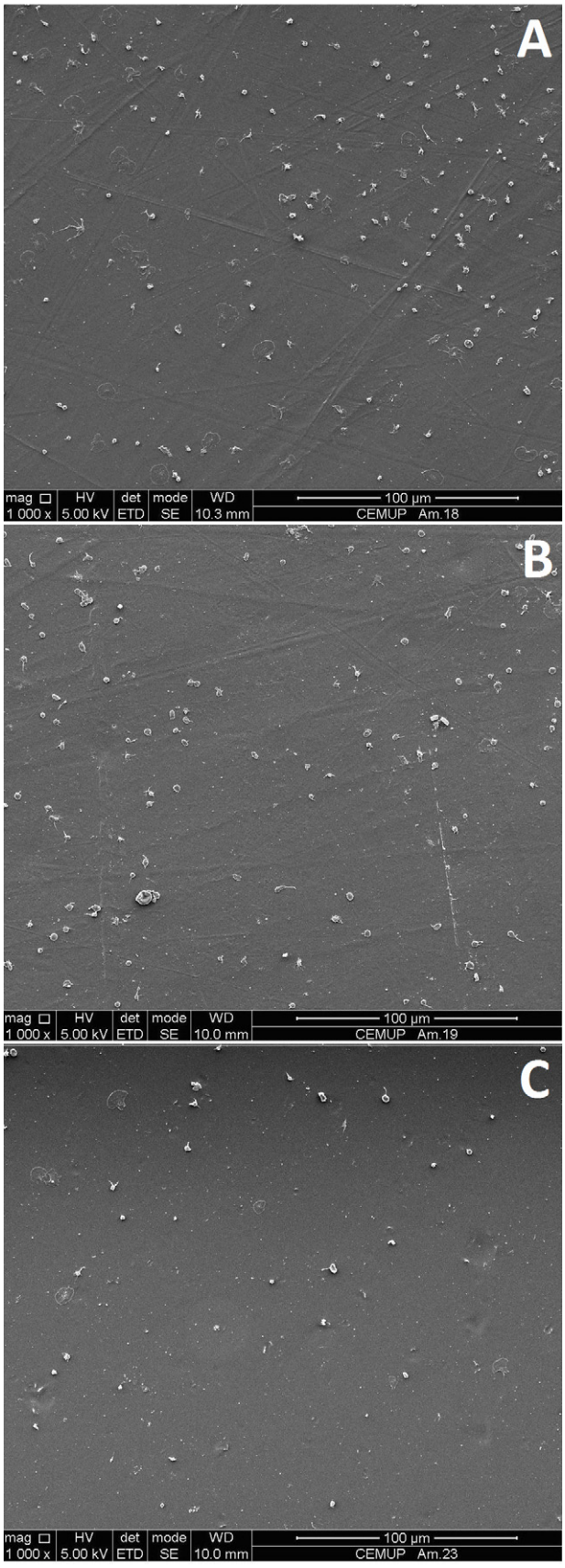

Fig. 11. Platelets adherent on the surface of PLA (A), PLA/GO and (B) PLA/GNP films pre-immersed in plasma (images of the films pre-immersed in PBS are not shown).

A decrease of platelet adhesion and activation after pre immersion in plasma has been previously described for surfaces that preferentially adsorb albumin over other plasma proteins [45,46]. Also, Koh et al. observed decreases in platelet adhesion and activation in (PLGA) poly(lactic-co-glycolic-acid) films pre-immersed in fibrinogen and non-stimulated rich plasma, whose surface was coated with multi-walled nanotubes, comparing to PLGA films without MWCNTs at the surface [34].

4. Conclusions

Incorporation of 0.4 wt.% loadings of GO and GNP changed the surface topography and wettability of PLA composite films. However, no considerable variation in cell proliferation at the surface of the films was observed, except for those containing GO after 24 h incubation, which presented a CPII inferior to pristine PLA films ($p < 0.05$). The presence of GO on the films surface may favor cell adhesion and proliferation due to creation of a more suitable surface morphology or to the increase in surface hydrophilicity. In the direct contact assay differences in morphology were not found for cells on the films surfaces or on the negative control (agar) surfaces. Moreover, all cells remained alive. Thus, it can be concluded that the films showed no cytotoxicity.

Mouse embryo fibroblasts incubated along time with different concentrations of GO and GNP did not present significantly different CPII values ($p > 0.05$), exceeding the IC_{50} with a concentration of 10 $\mu g\,mL^{-1}$.

The number of activated platelets in PLA/GNP films is significantly lower than for pristine PLA films ($p < 0.05$) in the presence of plasma.

These results indicate that small amounts of GO and GNP can be safely incorporated in PLA to improve its mechanical properties for biomedical applications. Additionally, GO has apparently a positive effect on cell adhesion and proliferation, leading to faster tissue regeneration. GNP incorporation, on the other hand, decreases thrombogenicity, which might reduce post operative complications caused by blood clots formation.

Acknowledgements

Funding for this work was partially provided by FEDER, through Programa Operacional Factores de Competitividade – COMPETE, and by National Funding through FCT – Fundação para a Ciência e a Tecnologia, in the framework of project PTDC/EME-PME/114808/2009 and of grant SFRH/BPD/63722/2009.

References

[1] R. Drumright, P. Gruber, D. Henton, Adv. Mater. 12 (2000) 1841.
[2] H. Tian, Z. Tang, X. Zhuang, X. Chen, X. Jing, Prog. Polym. Sci. 37 (2012) 237.
[3] S. Ramakrishna, J. Mayer, E. Wintermantel, K.W. Leong, Compos. Sci. Technol. 62 (2001) 1189.
[4] I. Armentano, M. Dottori, E. Fortunati, S. Mattioli, J.M. Kenny, Polym. Degrad. Stab. 95 (2010) 2126.
[5] B.D. Ratner, A.S. Hoffman, F.J. Schoen, J.E. Lemons (Eds.), Biomaterials Science, First Edition: an Introduction to Materials in Medicine, Academic Press, San Diego, CA, 1996, ISBN: 0-12-582460-2.
[6] L. Cabedo, J. Feijoo, M. Villanueva, J. Lagarón, E. Giménez, Macromol. Symp. 233 (2006) 191.
[7] S.D. Park, M. Todo, K. Arakawa, M. Koganemaru, Polymer 47 (2006) 1357.
[8] M. Murariu, A. Ferreira, M. Pluta, L. Bonnaud, M. Alexandre, P. Dubois, Eur. Polym. J. 44 (2008) 3842.
[9] J.H. Chang, A. Yeong, G. Sur, J. Polym. Sci. B 41 (2003) 94.
[10] C. Wu, H. Liao, Polymer 48 (2007) 4449.
[11] V. Mittal, Materials 2 (2009) 992.
[12] H. Kim, A.A. Abdala, C.W. Macosko, Macromolecules 43 (2010) 6515.
[13] A.M. Pinto, J. Martins, J.A. Moreira, A.M. Mendes, F.D. Magalhães, Dispersion of graphene nanoplatelets in PVAc latex and effect on adhesive bond strength, Polym. Int., in press.
[14] D.R. Dreyer, S. Park, C. Bielawski, R.S. Ruoff, Chem. Soc. Rev. 39 (2010) 228.
[15] L. Zhang, J. Xia, Q. Zhao, L. Liu, Z. Zhang, Small 6 (2010) 537.
[16] K. Yang, S. Zhang, G. Zhang, X. Sun, S.T. Lee, Z. Liu, Nano Lett. 10 (2010) 3318.
[17] A. Kumari, S.K. Yadav, S.C. Yadav, Colloids Surf. B 75 (2010) 1.
[18] H. Bai, C. Li, G. Shi, Adv. Mater. 23 (2011) 1089.
[19] M. Pumera, Chem. Rec. 9 (2009) 211.
[20] M. Kalbacova, A. Broz, J. Kong, M. Kalbac, Carbon 48 (2010) 4323.
[21] Y. Wang, Z. Li, J. Wang, J. Li, Y. Lin, Trends Biotechnol. 29 (2011) 205.
[22] X. Zhang, J. Yin, C. Peng, W. Hu, Z. Zhu, W. Li, et al., Carbon 49 (2011) 986.
[23] Y. Chang, S.T. Yang, J.H. Liu, E. Dong, Y. Wang, A. Cao, et al., Toxicol. Lett. 200 (2011) 201.
[24] P. Begum, R. Ikhtiari, B. Fugetsu, Carbon 49 (2011) 3907.
[25] D. Lahiri, R. Dua, C. Zhang, I. Socarraz-Novoa, A. Bhat, S. Ramaswamy, A. Agarwal, ACS Appl. Mater. Interfaces 4 (2012) 2234.
[26] M. Wojtoniszak, X. Chen, R.J. Kalenczuk, A. Wajda, J. Lapczuk, M. Kurzewski, et al., Colloids Surf. B: Biointerfaces 89 (2012) 79.
[27] J. Wang, P. Sun, Y. Bao, J. Liu, L. An, Toxicol. In Vitro 25 (2011) 242.
[28] O.N. Ruiz, K.A. Fernando, B. Wang, N.A. Brown, P.G. Luo, N.D. McNamara, M. Vangsness, Y.P. Sun, C.E. Bunker, ACS Nano 5 (2011) 8100.
[29] Y. Pan, T. Wu, H. Bao, L. Li, Carbohydr. Polym. 83 (2011) 1908.
[30] P. Song, Z. Cao, Y. Cai, L. Zhao, Z. Fang, S. Fu, Polymer 52 (2011) 4001.
[31] Y. Cao, J. Feng, P. Wu, Carbon 48 (2010) 3834.
[32] S.C. Tjong, eXPRESS Polym. Lett. 6 (2012) 437.
[33] C.J. Wilson, R.E. Clegg, D.I. Leavesley, M.J. Pearcy, Tissue Eng. 11 (2005) 1.
[34] L.B. Koh, I. Rodriguez, J. Zhou, J. Biomed. Mater. Res. A 86 (2008) 394.
[35] A.M. Pinto, J. Cabral, D.P. Tanaka, A.M. Mendes, F.D. Magalhães, Effect of graphene oxide and graphene nanoplatelets incorporation on mechanical and gas permeability properties of poly(lactic acid) films, Polym. Int. 62 (2013) 33.
[36] H. Fukushima, Graphite nanoreinforcements in polymer nanocomposites, Ph.D. Thesis, Michigan State University, 2003.
[37] K. Kalaitzidou, H. Fukushima, H.L. Drzal, Composites A 38 (2007) 1675.
[38] D. Tanaka, A.M. Mendes, Composite graphene-metal oxide platelet method of preparation and applications, International Patent No. PCT/IB2010/055598, 2010.
[39] E.S. Gadelmawla, M.M. Koura, T.M. Maksound, I.M. Elewa, H.H. Soliman, J. Mater. Process. Technol. 123 (2002) 133.
[40] M. Sedlaček, B. Podgornik, J. Vižintin, Tribol. Int. 48 (2012) 102.
[41] J. Wang, X. Wang, C. Xu, M. Zhang, X. Shang, Polym. Int. 60 (2011) 816.
[42] O.J. Yoon, C.Y. Jung, I.Y. Sohn, H.J. Kim, B. Hong, M.S. Jhon, N.E. Lee, Composites A 42 (2011) 1978.
[43] A.C. Vieira, J.C. Vieira, F.M. Ferra, F.D. Magalhães, Guedes R.M, A.T. Marques, J. Mech. Behav. Biomed. Mater. 4 (2011) 451.
[44] L. Vroman, A.L. Adams, J. Biomed. Mater. Res. 3 (1969) 669.
[45] I.C. Gonçalves, M.C. Martins, J.N. Barbosa, P. Oliveira, M.A. Barbosa, B.D. Ratner, J. Mater. Sci. Mater. Med. 22 (2011) 2053.
[46] I.C. Gonçalves, M.C.L. Martins, M.A. Barbosa, E. Naeemi, B.D. Ratner, J. Biomed. Mater. Res. A 89 (2009) 642.